

Computational Analysis of Ground Effects on the Dynamical Behavior of Unconfined Two-Phase Clouds in View of Detonability Studies

K. Mazaheri*, M.M. Doustdar¹ and M. Hosseinalipour²

A numerical analysis has been performed to investigate the ground effects on the main parameters of a two-phase unconfined cloud of fuel and air to study its detonability. Equivalence ratio, turbulence intensity, cloud shape and volume, uniformity, temperature gradient and delay time distribution are the most important factors that affect the detonability of a vapor cloud. The effects of the altitude of the dispersing device from the ground on these significant factors have been demonstrated. A modified KIVA-based program has been employed to carry out the computations. A finite volume method is used to solve the equations describing the gas phase. A discrete particle technique is applied to represent the liquid spray and a $k - \varepsilon$ model is used for modeling the gas phase turbulence. Theoretical considerations and comparison with associated experimental values were made for validation. As the injection height increases, the cloud becomes more uniform and the possibility of the pulsing propagation of the detonation wave decreases. When the injection height decreases, the contour of the detonable range rotates faster and delay time decreases. As a trade-off between all effective parameters, in this paper, an optimum for the injection height is introduced.

INTRODUCTION

When a combustible gas or evaporating liquid escapes accidentally into an open atmosphere, a combustible cloud of fuel and air may form. If the cloud is within flammability limits, an ignition will lead to the propagation of a combustion wave through the flammable parts of the cloud. The mode of combustion may be deflagration or detonation. Although the most likely scenario is a weak ignition source, like a hot surface or a spark and, then, the propagation of a deflagration wave, in proper conditions, a detonation wave may propagate through the cloud. Because of the large overpressure and remarkable impulse, a

detonation is the most severe type of explosion in a mixture of fuel and air. It can result in huge loss of property, as well as injuring people. The behavior of a detonation wave, especially in an unconfined mixture, is completely different from that of a deflagration wave. A detonation wave does not require confinement or obstruction to propagate at a high velocity [1]. In spite of much valuable information that has been incorporated into practical guidance for industry, many problems have still remained and there are a lot of serious explosions each year. Preventing such events from happening requires a good knowledge of gas explosion and the way of reducing the frequency and consequence of its occurrence. By studying detonation in unconfined clouds, an understanding about what detonation is and how it may be initiated can be improved upon.

Direct initiation of detonation and its propagation through an unconfined cloud, as well as the transition of deflagration to detonation, depend strongly on the reactivity of the cloud. Some characteristic parameters of the cloud, such as its shape and volume, growth rate and fuel concentration distribution, have a great

*. Corresponding Author, Department of Aerospace Engineering, Sharif University of Technology, Tehran, I.R. Iran.

1. Department of Aerospace Engineering, Sharif University of Technology; Department of Mechanical Engineering, Imam Hossein University, Tehran, I.R. Iran.
2. Department of Mechanical Engineering, Iran University of Science and Technology, Tehran, I.R. Iran.

influence on the degree of reactivity and, hence, on the mode of propagating the combustion wave. Also, the location of the ignition point and the strength and type of the ignition source play a significant role in detonation initiation.

Many studies have aimed at investigating the initiation of detonation in unconfined clouds and at modeling combustion in two-phase flows. Alekseev et al. [2] experimentally studied the detonation of a large-scale unconfined fuel spray. They studied the effects of cloud size, type of fuel and mass of explosive charge on the detonability of a cloud. Benedick et al. [3] performed some tests to investigate the detonability of some types of fuel and demonstrated the possibility of detonation in a two-phase state for some kinds of fuel. Thomas et al. [4] represented some observations of detonation initiated by a jet of combustion products. Their results showed that significant unconfined flame acceleration could occur in an appropriate large volume. Moreover, the increase in energy release rate in a turbulent reaction front could lead to auto-ignition conditions in pockets of the unburned mixture. Ungut et al. [5] also studied, experimentally, the deflagration to detonation transition. All their experimental results, for a given initial pressure and fuel, may be collapsed to a single curve, separating conditions leading to detonation from those which do not. They suggested a criterion, based on the notation of a critical Damkohler number and minimum energy release requirement, for the initiation of unconfined detonation by a venting jet flame. The critical initiation energy and explosion limits of some hydrocarbon-air mixtures were measured by Lizhong et al. [6] in confined and unconfined condition tests. Doustdar et al. [7] introduced a numerical simulation to study the behavior of a two-phase cloud of fuel and air, for stagnant and moving air. In the moving case, they considered an initial velocity for the dispersing device. Bartenev et al. [8] described the process of detonation initiation within the scope of the spontaneous flame concept. They believed that the origin of certain combustion modes was conditioned by the gradients of self-ignition delay time in the system. Khokhlov et al. [9] have discussed the role of shock-flame interactions in turbulent flames in their numerical simulation of deflagration to detonation transition. Makhviladze et al. [10] have considered, numerically, the formation, evolution and combustion of two-phase clouds in an open atmosphere. In their work, transient axisymmetric flows occurring upon the finite-duration vertical release of pressurized-liquefied gases were studied numerically. Glass [11] performed a numerical simulation for the far-field regime of fuel-air explosive devices. He used the KIVA-II code for his calculations.

In the present work, by modifying a KIVA-3 based code, a numerical simulation was reformed to study the

ground effects on the main parameters that influence the detonability of two-phase unconfined clouds. The dispersing device, used to produce the unconfined fuel and air cloud, is shown in Figure 1. In this device, some liquid fuel is initially considered inside a cylindrical container. Then, by the explosion of a small burster charge along the axis of the container, as shown in Figure 1, the container will be broken up and the fuel will be dispersed into the open atmosphere. To simulate the explosive dispersal of the liquid fuel from such a cylindrical container, a multi-nozzle modeling has been introduced and applied. In this model, a large number of imaginary nozzles with small spray cone angles are considered along the dispersing device. The fuel particles come into the field from these nozzles. Because of symmetry assumption, the angle of injection for each nozzle in the azimuthal direction is 360° . By changing the distance of the dispersing device from the ground, the influence of the ground could be studied, as a solid boundary, on the final dynamical behavior of the cloud. Main computation starts when the fuel is fully broken up into discrete droplets. The basic objective of this work is to investigate how the ground affects the main detonability characteristics of the cloud and, hence, how it changes the proper ranges of time and position for igniting a cloud to initiate detonation. A comparison is made between these numerical results and the relevant experimental results for validation purposes. These results may also be useful for the formulation of safety procedures and regulations regarding liquid fuel storage.

MAIN CHARACTERISTIC PARAMETERS

Based on the relative magnitude of the inertia and aerodynamic forces acting on the fuel, the dispersion pro-

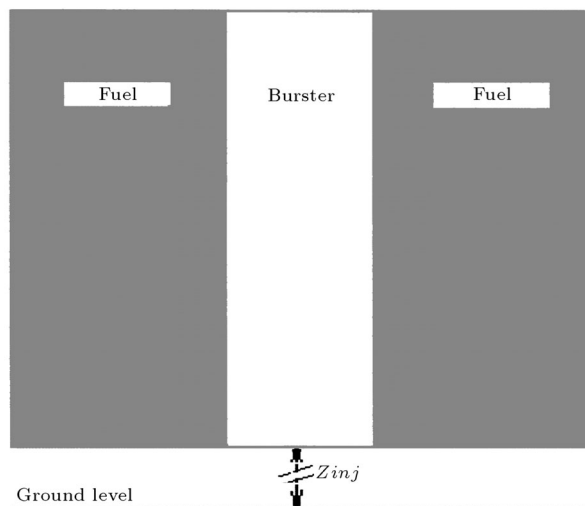


Figure 1. Schematic diagram of the dispersing device.

cess can be divided into three regimes. The first is the ejection regime, in which the inertia forces dominate the aerodynamic forces. The second is the transition regime, in which the inertia and aerodynamic forces are approximately of the same magnitude. The third is the expansion regime, in which the aerodynamic forces dominate the inertia forces and the concentration of the fuel inside the cloud is relatively low. Because the expansion regime constitutes most of the final volume of the cloud, this regime predominantly controls the final characteristics of the cloud [11]. Therefore, by numerical simulating of this regime, one may be able to quantitatively analyze the important parameters of the cloud. To improve the reliability of the detonation formation, one needs to understand the mechanism of fuel dispersal and the factors that influence the cloud behavior.

When a flame propagates through a premixed cloud, fast propagation and burning in confined volume are the most important mechanisms causing pressure build-up [1]. As a result, in an unconfined premixed cloud, the pressure is strongly linked to the burning rate and flame velocity or the reactivity of the cloud. Some parameters of the cloud, such as size, shape, growth rate, uniformity and the distributions of turbulence intensity, equivalence ratio, thermodynamic properties and droplet size, as well as the fuel type, play the main roles in determining the reactivity of the cloud and in designating the mode of combustion which propagates through it.

Due to higher molecular diffusivity and fast chemical kinetics, some fuels have higher burning velocity. Furthermore, a premixed cloud of fuel and air will only detonate as long as the equivalence ratios inside it are within detonability limits. Generally, when fuel concentration is near flammability limits, burning rate will be very low [1].

Turbulence in the cloud is another important factor. When a flame propagates into a turbulent flow field, the burning rate will increase significantly. This increment in burning rate will further increase both the turbulence ahead of the flame and the flow velocity [1]. This powerful positive feedback mechanism will cause flame acceleration, high explosion pressure and, in proper conditions, can produce detonation.

The volume and shape of the cloud are also important parameters. To generate a stable detonation, the cloud size should be much greater than the detonation cell size. The cell size is a measure of the reactivity of the mixture. In fact, the cell size is a length scale characterizing the overall chemical reaction in the detonation wave. For a more reactive mixture, the cell size is smaller [1]. Experimental results indicate that near the critical size of a cloud, a pulsing behavior of the detonation wave is observed. A semi-empirical relation between detonation cell width, λ , and critical

radius, R_c , was given by Alekseev et al. [2], as follows:

$$R_c = (8 - 12)\lambda. \quad (1)$$

The radius of the cloud must be long enough to support the detonation wave and bring it up to strength. The impulse and duration of the positive pressure phase depend on the size of the cloud.

The growth rate and shape of the cloud are the most remarkable parameters in evaluating the proper time for the ignition. These parameters, together with the total mass of fuel, determine the bulk density of the cloud and the fuel concentration. Furthermore, the uniformity of the cloud has a considerable effect on the efficiency of the consequent detonation, as well as on the uniformity of the subsequent blast wave. In addition, both the strength of the detonation wave and the direction of its propagation are influenced by the droplet size distribution. The temperature gradients inside the cloud play an important role in designating the mode of combustion that propagates through the cloud. Besides that, igniting the cloud at a proper time and in a suitable position has a great influence on detonation initiation. The explosion pressure can be very sensitive to the location of the ignition point. In many cases, moving the ignition location from the worst point to a more suitable position can vary the peak pressure of the explosion by an order of magnitude [1]. The time and position of the ignition affect the combustion energy release and the latter plays a role in determining the type of consequent blast wave.

NUMERICAL PROCEDURE

A modified KIVA-3 based code is used to perform the computations. Here, the numerical procedure is based on the viewpoints of the Discrete-Droplet Model (DDM). In this model, the entire spray is represented by finite numbers of groups of particles. Each particle represents a number of droplets of identical size, velocity and temperature. A Lagrangian formulation is used to track the motion and transport of particles through the flow field and a Eulerian formulation is used to solve the governing equations for the gas phase. The effects of droplets on the gas phase are considered by designating proper source terms in the gas phase conservation equations. The particles and gas interact by exchanging mass, momentum and energy. For assigning droplet properties at injection or anywhere in downstream, a probability concept is applied. A Monte Carlo sampling technique is used to calculate droplet properties. Droplet collision and breakup are also considered in each computational time step. The gas phase solution procedure is based on the ALE (Arbitrary Lagrangian-Eulerian) finite volume method.

The basic equations are differenced in integral form. A typical cell is used as the control volume. The divergence terms are transformed to surface integrals using the divergence theorem. A standard version of the $k - \varepsilon$ turbulence model has been used. The turbulent law of the wall is employed to calculate wall heat transfer and boundary layer drag. More description is well documented in [12,13].

However, necessary modifications have been carried out pertaining to the calculation of the characteristic parameters of an unconfined cloud. In fact, the original code can be divided into three major segments: (1) The pre-processor; (2) The computational model; and (3) The post processor. Because KIVA was originally developed to model internal combustion engines, it incorporated many codes that were very specific towards this task, such as the grid generation routines, piston and valve movement and fuel injection. These routines were removed and replaced with some routines which were specifically coded to handle unconfined cloud modeling. The pre-processor segment was modified to serve input data related to an unconfined dispersal, like the dispersing device altitude, the fuel explosive limits, and so on. Some routines have been added to the computational segment to calculate the equivalence ratio distribution, the volume of the detonable range, the height and radius of the cloud, the circulation around the vortices inside the flow field, the delay time and temperature gradient distributions, the variance of density and equivalence ratio, the mean and maximum turbulent kinetic energy of the cloud and so on. The post processor segment was modified to provide output files compatible with common graphics codes, especially TECPLOT. Evidently, some controlling commands were removed or replaced as well. A multi-nozzle modeling has also been introduced to simulate the dispersal of the fuel from cylindrical containers.

DOMAIN OF COMPUTATION AND BOUNDARY CONDITIONS

Based on the injection initial conditions, the dimensions of the domain of computation are determined. As the injection height, total fuel mass and injection velocity increase, a larger domain of computation should be considered. Because of azimuthal symmetry assumption, as well as for saving computation time, a small sector has been chosen as the domain of computations. The rectangular mesh generated for the computational domain is shown in Figure 2. As the boundary conditions, "axis" was applied for the axis of symmetry, "pressure outflow" for the circumferential side, "solid" for the bottom, "pressure inflow" for the top, and "periodic front" and "periodic derriere" for the azimuthal directions [13].

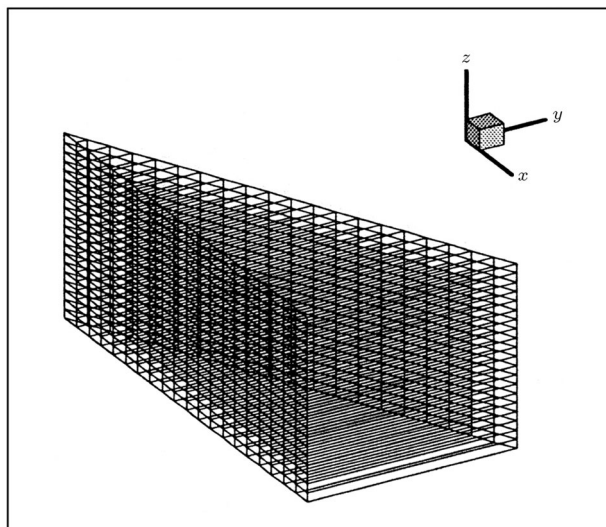


Figure 2. The computational grid.

RESULTS AND DISCUSSIONS

In this section, some typical results are presented. Here, changes in equivalence ratio field, velocity vector field, turbulent flow scales and thermodynamic property distributions have been studied, as well as the volume, shape and uniformity of the cloud with time. Studies have been made on how the ground affects these fields and variables. The most important physical phenomena involved in such a problem have been taken into account, like the collision, coalescence, breakup and evaporation of spray drops. The main fuel was gasoline with a total mass of 15 kg. The height and diameter of the cylindrical dispersing device, depicted in Figure 1 and the initial injection velocity were 0.48 m, 0.3 m and 250 m/s, respectively. Using the injection velocity and the device diameter, the injection duration could be computed [11,14]. A \mathcal{X} -squared distribution function with a Sauter mean radius of 1 cm was also applied [14,15] to assign the diameter of each injected particle by a stochastic method [12]. All the units are in SI. In the presented figures, "Time" is the time after the injection and " Z_{inj} " is the injection height, which is the distance of the bottom of the dispersing device from the ground (Figure 1).

Velocity Vector Field

When the fuel is injected into the open atmosphere, two relatively strong vortices will form and develop inside the produced vapor cloud. The lower vortex, as shown in Figure 3a, rotates in a clockwise direction and the upper one rotates inversely. These vortices have a great effect on the distributions of the other interested variables. Because of the ground effect, the lower vortex decays faster. Then, the entire flow field is induced by the strength of the upper vortex (Figure 3b). However, as the distance of the dispersing

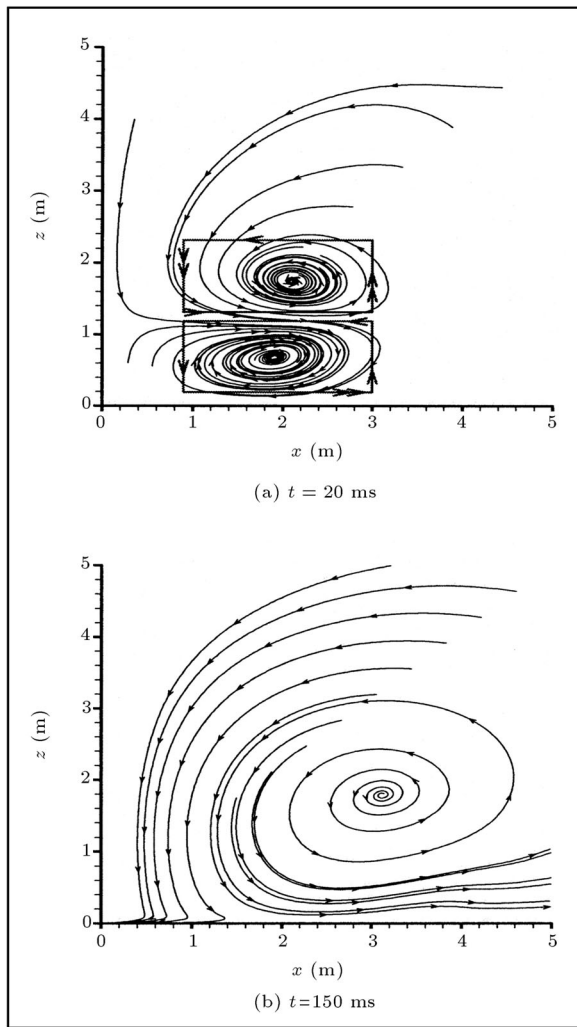


Figure 3. Flow streamlines at $Z_{inj} = 1$ m. The rectangles in (a) depict the chosen paths for taking circulation.

device from the ground (the injection height) increases, the ground effect diminishes and the lower vortex continues rotating as the upper one.

To evaluate the effects of the injection height on the strength of the vortices and to predict the decay time of the lower one, the circulation is considered around these vortices. Circulation is simply the line integral of velocity around a closed curve (c) in the flow, defined as:

$$\Gamma = \oint_c \mathbf{v} \cdot d\mathbf{s}. \quad (2)$$

Vector \mathbf{v} is velocity and vector $d\mathbf{s}$ is directed line segment. Circulation is a kinematic property depending only on the velocity field and the choice of the curve, c . The circulation, Γ , around a vortex is equal to the strength of the vortex. Hence, when the circulation about the lower vortex is about zero, this vortex is damped away. This determines the decay time of

the lower vortex. Figure 4 shows the variations of the circulation around the lower vortex in time for different injection heights. The circulation, as shown in Figure 3a, was taken on a rectangular path. Because of the difference in the injection height for the compared cases, the rectangular paths enclosing the lower vortex have different widths. Thus, to make the circulation around different paths comparable, the circulation per unit area was calculated. To show the decay time, zero was chosen as the upper limit of the vertical coordinate. By mathematical convention, the positive sense of the line integral is counterclockwise. Since the lower vortex rotates clockwise, the value of the circulation about it is negative. This figure depicts that, as the injection height increases, the lifetime of the lower vortex increases. For instance, when the injection height is 3 m, the lower vortex continues rotating even after $t = 0.25$ s. Furthermore, in the earlier stages of time, for a smaller injection height, the absolute value of the vortex strength is larger. Figure 5 shows the variations of the circulation with time around the upper vortex at different injection heights. Here, the rectangular paths have equal widths. As the injection height increases, the strength of the upper vortex decreases. That is because of the ground effects on the flow field. Taking circulation on a path embedding both vortices simultaneously, as shown in Figure 6, results in the net strength. Figure 6 shows that as the injection height increases, the strengths of the lower and upper vortices will be closer to each other, so that the net strength converges towards zero and, hence, the cloud goes towards more symmetry.

The position of the ignition, with respect to the centers of the vortices, is of great importance. If the ignition happens close to the center of one of these vortices, the laminar propagation of combustion

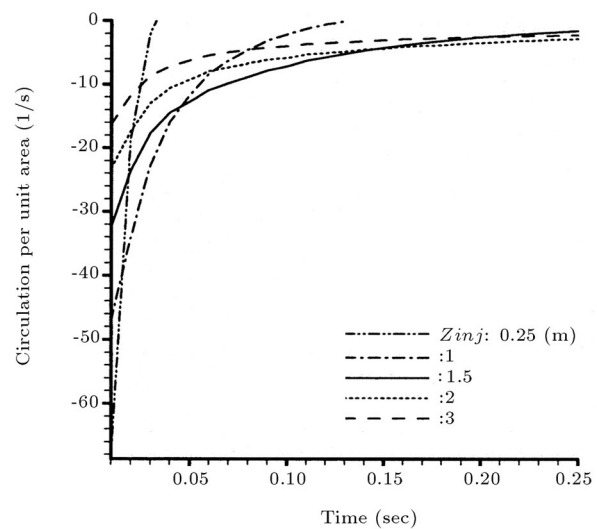


Figure 4. Variations of the circulation per unit area around the lower vortex at different injection heights.

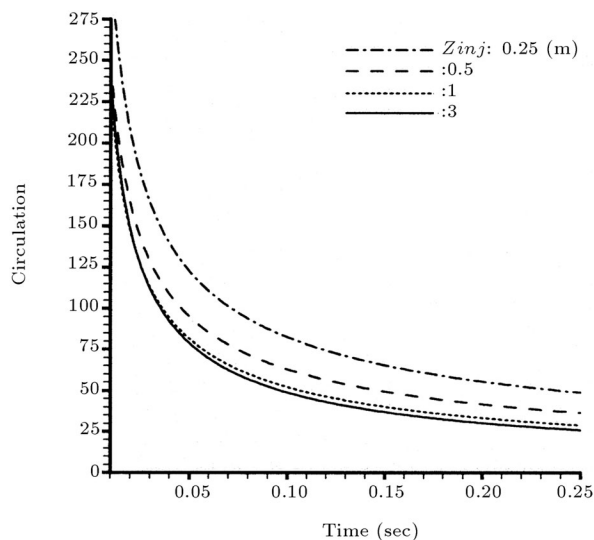


Figure 5. Variations of the circulation (m^2/s) around the upper vortex at different injection heights.

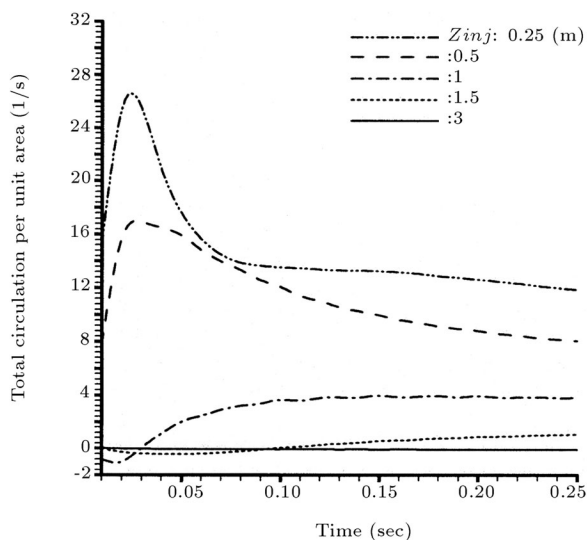


Figure 6. Variations of the net circulation per unit area around the vortices at different injection heights.

precedes the turbulent one. But, if the ignition occurs in the periphery of one of them, then, the turbulent propagation precedes the laminar one. In the latter case, the rate of combustion increases and a relatively stronger detonation wave is expected. From a turbulence point of view, the common region between the two vortices is a very suitable position for the ignition action and has the potential for initiating a stronger detonation wave. It seems that the initiation of an unconfined detonation is closely related to a high rate of energy release ensuing from intense combustion inside the above-mentioned unburned vortex. Because of the favorable pressure differential, the hot combustion products are sucked rapidly towards the center of the vortex. Then, a rapid mixing of the unburned mixture with the combustion products leads to a strong

combustion. According to the available experimental evidence [5], both the rate of energy release and the flame speed rise notably for such an interaction. The numerical studies by Khokhlov et al. [9] have also confirmed the significant influence of increase in the local rate of reactions on the formation of hot spots and the final transition to detonation. The ratio of the time scale of the suction of combustion products into the vortex to that of the chemical reactions is a criterion for a successful transition to unconfined detonation [5]. A large value of this ratio, which can be interpreted as a Damkohler number, means that the suction and mixing of the combustion products happen during a relatively longer time scale than that of the chemical induction time. Consequently, the rate of energy release is low. In contrast, as this ratio decreases, the suction and mixing of the combustion products occur in a relatively shorter time scale than that of the chemical induction time. This is followed by explosive combustion and a high rate of energy release. As the turbulent kinetic energy increases, this ratio decreases [5] and there will be more possibility of detonation. Figure 7 represents the variations of the mean turbulent kinetic energy for different injection heights. This energy diminishes gradually in time and, hence, from this point of view, earlier stages of time are seemlier for igniting the cloud. This figure also indicates that there is an optimum injection height, which has, relatively, the largest value of mean turbulent kinetic energy.

Equivalence Ratio Field

Figure 8 shows the Equivalence Ratio (ER) field for $Z_{inj} = 1$ m at $t = 20$ ms and $t = 200$ ms. In computing the equivalence ratio, only the mass of vaporized fuel was used. The outer contours of the

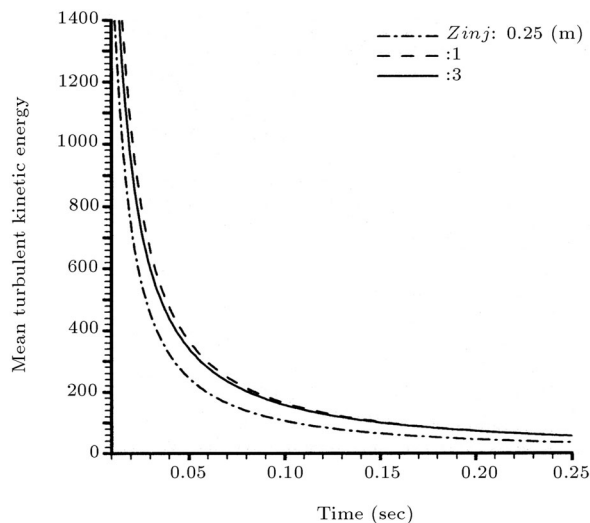


Figure 7. Variations of the mean turbulent kinetic energy (J/kg) at different injection heights.

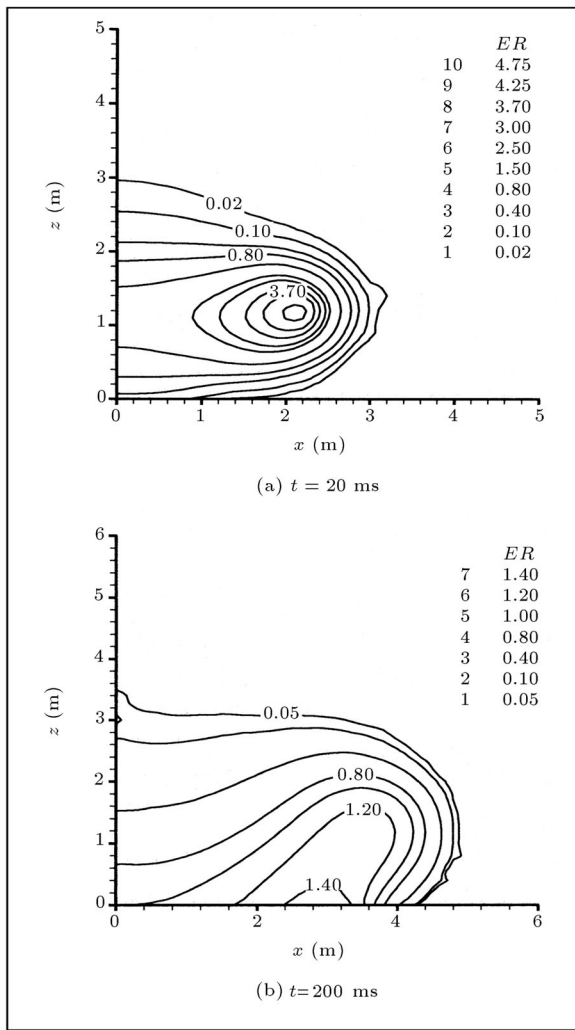


Figure 8. Equivalence Ratio (ER) field at $Z_{inj} = 1$ m.

equivalence ratio indicate the volume and shape of the cloud. By comparing the equivalence ratio field at various times, one can calculate the growth rate of the cloud. Since the range of detonability of gasoline is almost between 0.8 and 3.7, the equivalence ratio field represents the suitable domain for the detonator action at a selected time. It is important to note that the required amount of energy for a successful ignition is also a function of the equivalence ratio [6]. Thus, by analyzing the ER field, one will be able to determine the amount of energy required for igniting the cloud in a proper position and time.

The volume of the detonable range is called the “effective volume”. Figure 9 represents the changes in the effective volume with time. Effective volume is the net result of two competing aspects, i.e., increased by droplet evaporation and decreased by cloud expansion. Thus, as shown in Figure 9, it will reach its maximum after some time and then decrease. As the injection height increases, at first, the effective volume increases and then decreases. As a result, from this point of view,

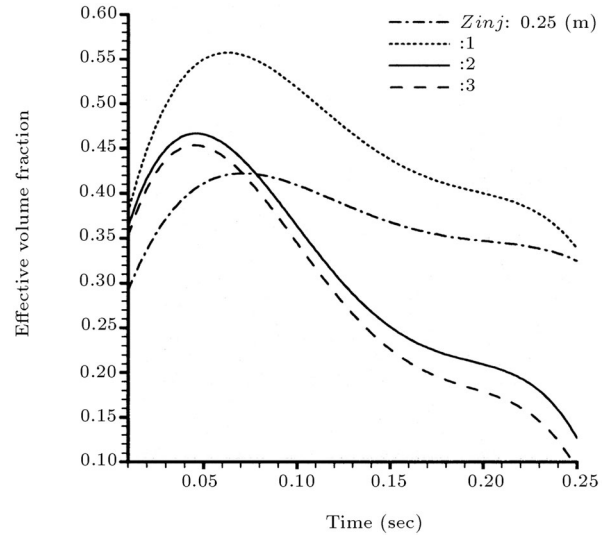


Figure 9. Variations of the effective volume fraction.

there is also an optimum value for the injection height. The available time window for successful initiation of detonation in unconfined clouds is generally very narrow. Every ignition system, on the other hand, has its own delay time. Therefore, when the effective volume has high values, there is more opportunity, i.e. position and time, for igniting the cloud with a specified amount of energy. A cloud with a higher effective volume is less sensitive to the precision of the ignition timing.

Figure 10 represents the changes in the variance of equivalence ratio with respect to stoichiometric composition ($ER = 1$) in time. The equation used to compute variance is [16] as follows:

$$S^2 = \frac{1}{n-1} \sum_{j=1}^n (ER_j - \overline{ER})^2, \quad (3)$$

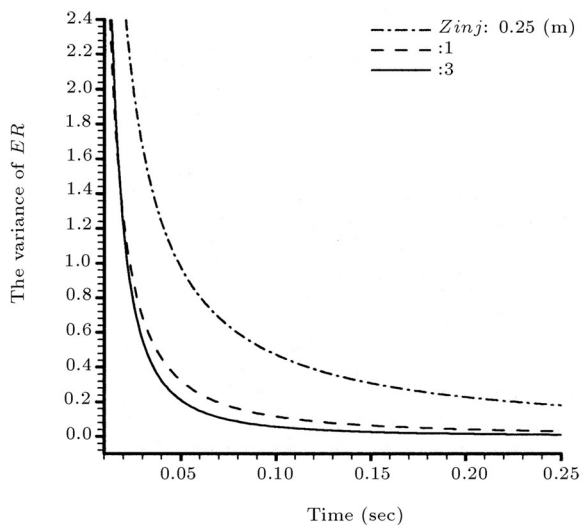


Figure 10. Variations of the ER variance with respect to $ER = 1$ at different injection heights.

S^2 is variance, ER_j is equivalence ratio in each computational cell, \overline{ER} is the average value of ER over the computational cells and n is the number of computational cells. In driving Figure 10, only the cells inside the effective volume were considered and \overline{ER} was replaced with 1. For more mixtures of fuel and air, variation in critical initiation energy with composition takes the form of a U-shaped curve with a minimum near the stoichiometric composition [17]. Furthermore, the maximum explosion pressure is normally observed at a stoichiometric or slightly rich mixture [1]. Therefore, the time when the variance goes towards zero is a suitable time for igniting the cloud to consume comparatively less initiating energy and to obtain more overpressure. The shape of the ensuing detonation and the direction of its propagation will be influenced by the uniformity of the equivalence ratio. This figure also demonstrates that the gradients of the equivalence ratio are larger in the earlier stages of time and then decrease. Furthermore, the gradients are smaller for larger injection heights. These gradients can pulsate the consequent detonation wave. Therefore, increasing the injection height will reduce the possibility of the pulsation in the propagation of the detonation wave.

Figure 11a shows that not only does the effective volume shift towards right but also rotates counter-clockwise. Thus, the detonable region moves gradually from left to right and from top to bottom and, hence, just after a short time, most of the area near the dispersing device will not be located in the detonable range. This phenomenon occurs when the lower vortex has been decayed, so that the entire flow field is induced by the upper vortex, which rotates counterclockwise. Thus, when the injection height increases, the ground effect decreases and the contour of effective volume will not rotate. This conclusion is confirmed by Figure 11b, in which the injection height is 3 m.

Figure 12 depicts the variations in the radius of the cloud with time. The contour of $ER = 0.02$ was used to drive this figure. The cloud radius must be large enough to support and strengthen the initiated detonation. As expected, the cloud radius increases with time. Furthermore, when the injection height increases, the radius of the cloud slowly increases. However, the cloud radius is only a weak function of the injection height.

Temperature Gradient Distribution

The intrinsic mechanism that triggers a detonation is the formation and explosion of nonuniformly preconditioned regions of a mixture in which a spatial gradient of delay time (time to ignition) has been created. In the direct initiation of detonation, the initiating explosion is provided by an external high-energy source, for instance, a high explosive charge. Such explosions

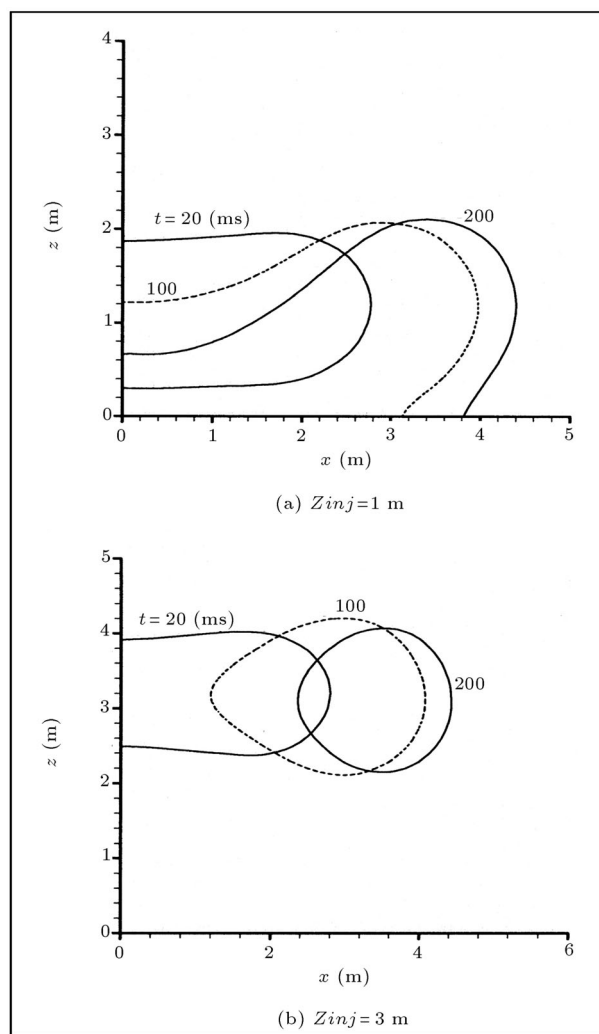


Figure 11. Contours of the effective volume.

produce strong shock waves, which initiate directly a self-sustained detonation. In transition to detonation, the energy required for the initiating explosion is provided by the combustion process itself. This self-initiation requires a rapid release of combustion energy to produce shock waves of sufficient strength to create detonation [17]. A prescribed spatial and temporal coherence of the energy release is required to produce such shock waves. The idea of spontaneous flame propagation, originally proposed by Zel'dovich, is useful to treat this coherence of the energy release. A spontaneous mode of flame propagation is a consecutive spontaneous release of chemical energy, which is not connected with the influence of gas dynamics processes [8]. In fact, the transition between different combustion modes is determined by the relationship between gas dynamical and chemical processes in the combustion wave. Spontaneous speed defines the chemical process part and shock waves or pressure waves are responsible for the gas dynamic part. The mode of combustion, which propagates through a

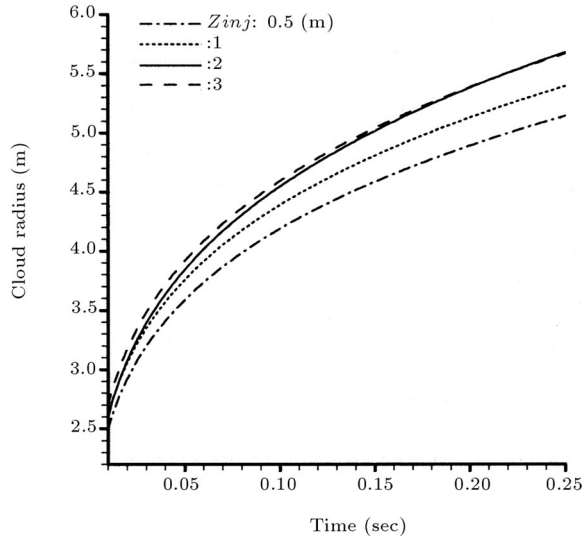


Figure 12. Changes in the radius of the cloud at different injection heights.

mixture, depends on the magnitude of spontaneous speed relative to the known speeds of combustion. A detonation is expected when the spontaneous speed is close to the $C - J$ detonation speed. The speed of spontaneous wave can be written [18] as:

$$D_{sp} = \left(\frac{\partial \tau}{\partial X} \right)^{-1}, \quad (4)$$

where τ is the delay time and X is the spatial variable. Delay time is a function of temperature and fuel concentration. Its spatial gradients are due to gradients in temperature and/or fuel concentration. Therefore, temperature gradients inside the cloud can determine the magnitude of the spontaneous speed and, hence, the detonability of the cloud. Only in a specified range of temperature gradient may a detonation be initiated inside a cloud. Out of this range, other modes of combustion will propagate through the cloud. Figure 13 shows the variations of the maximum of radial component (in X direction shown in Figure 2) of the temperature gradient. As the injection height increases, the temperature gradients decrease, so that the spontaneous wave can propagate faster and, hence, from this point of view, there is more possibility of detonation. By analyzing temperature gradient distribution, one can determine when all the temperature gradients inside the cloud are smaller than a specified limit. Combined with appropriate experimental results, such numerical results can help to find the required range of temperature gradient to detonate an unconfined cloud.

The above-mentioned initiating explosion generally starts at a point of minimum delay time. Figure 14 shows the changes of the minimum delay time for different injection heights. To compute the delay time distributions, the equation introduced in [8] was used

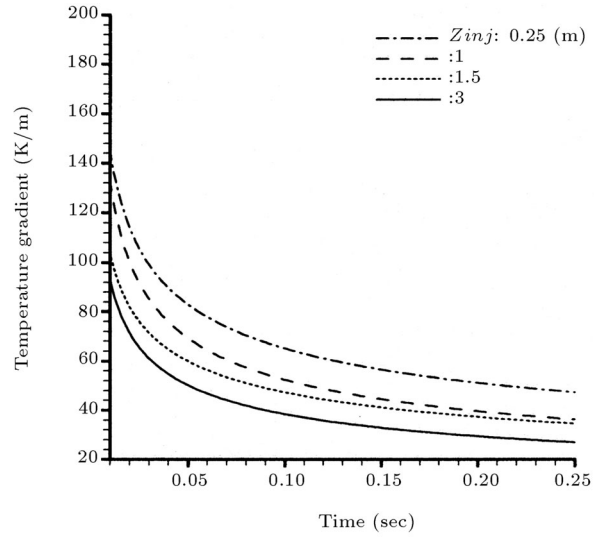


Figure 13. Variations of the maximum value of radial (in X direction) component of temperature gradient at different injection heights.

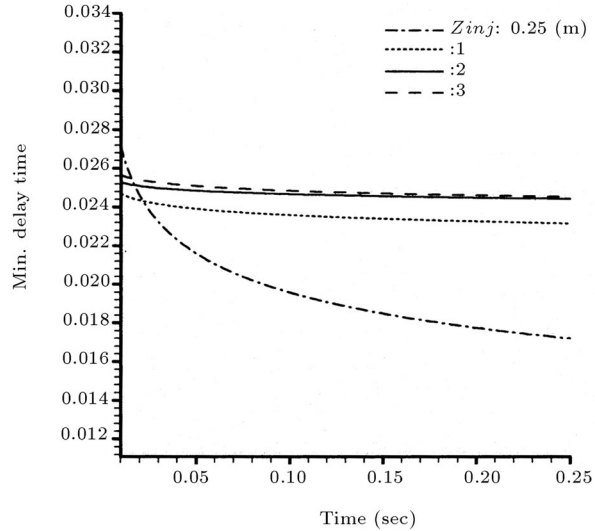


Figure 14. Variations of the non-dimensional delay time at different injection heights.

as follows:

$$\tau_i(x, y, z) = \frac{c_v R(T(x, y, z))^2 \exp(E/RT(x, y, z))}{f Q \lambda(x, y, z) E} \left[1 + \frac{2RT(x, y, z)}{E} \right], \quad (5)$$

C_V, E and f are: Specific heat at constant volume, activation energy and frequency factor in Arrhenius' law, respectively. Q, R, T and λ are: Heat of reaction, universal gas constant, temperature and fuel concentration, respectively. The less the delay time, the faster the detonation initiation. Figure 15 shows the location variations of the point with a minimum value of delay time. A linear curve fitting was applied to show the

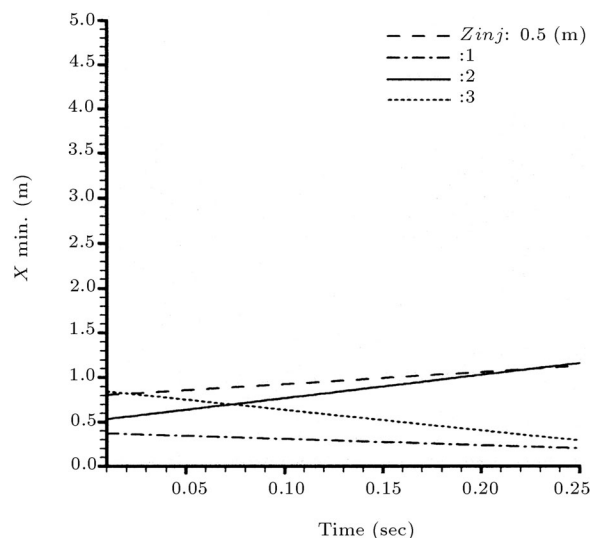


Figure 15. Changes in the location of minimum delay time point in time for different injection heights.

trend of variations. As shown, there is also an optimum injection height. As the location of this point orientates towards a smaller radius, more fuel may be consumed by the detonation, so that a stronger detonation wave and a higher efficiency can be expected.

EXPERIMENTAL TESTS

A limited number of experimental tests were performed to study cloud evolution, initiation of detonation and the effects of the created wave on surrounding equipment. The configuration of the dispersing device was cylindrical, with a central cylindrical burster charge surrounded by a cylindrical annulus of liquid fuel (see Figure 1). Some kinds of liquid fuel, especially gasoline, were used as the main fuel. C4 was used as the burster charge, to disperse the main fuel. Some indexes, glass tables and measuring instruments were used to observe and study the cloud formation and evolution, as well as the detonation effects on surrounding equipment. A high-speed camera with a framing rate of 2000 fps and a video camera were also implemented in suitable positions to record the whole process. Figure 16 shows, typically, three frames of the dispersion process and the propagation of the detonation. In this test, the injection height was 0.8 m and 15 kg of gasoline were used as the main fuel. The cylindrical container height and diameter were 0.40 m and 0.3 m, respectively.

Although the information inside the cloud is also important and interesting, up to now, it was unable to be obtained reliably from experimental tests. However, one can estimate the volume, shape, growth rate and height of the cloud by using high-speed films generated in these experiments. Hence, to partially validate the results of this numerical simulation, the variations of the radius of the cloud, calculated numerically, and the



(a) $t = 5$ ms



(b) $t = 10$ ms



(c) $t = 100$ ms

Figure 16. Pictures of the vapor cloud evolution and detonation at different times.

related experimental values, were compared. Figure 17 represents this comparison. In determining the cloud radius experimentally, the distance between the leading edge of the cloud and the axis of the dispersing device were measured. In the numerical approach, mainly, the contour of $ER = 0.02$ was used to determine the cloud radius. The experiences demonstrate that the contours of $ER \leq 0.1$ satisfactorily represent the edge of the cloud.

To estimate the injection velocity, it is assumed that 70 % of the burster explosion energy converts to the fuel kinetic energy [11]. The results of [15] also confirm this assumption. Based on this, it was found that:

$$V_{inj} = 0.1183(H_{exp}m_{rp})^{1/2}, \quad (6)$$

where H_{exp} is the specific enthalpy of explosion of the burster charge and $m_{rp} = (m_{bc}/m_f) \times 100$. m_{bc} and m_f are the burster and fuel masses, respectively.

It is observed from Figure 17 that the numerical method can predict the radius of the cloud fairly well. The consistency of the numerical and experimental curve slopes at different times is also fairly good. Therefore, the numerical simulation can estimate the growth rate of the cloud accurately. This figure demonstrates that the numerical and physical models [12,13], applied to simulate the liquid fuel dispersal and dynamical behavior of the unconfined cloud, work satisfactorily.

CONCLUSIONS

A numerical study has investigated the ground effects on the main parameters that influence the detonability of fuel and air clouds. The equivalence ratio, turbulence intensity, uniformity, temperature and delay time

gradients, as well as the volume, shape and growth rate of the cloud, were introduced as the most important parameters to influence the detonability of an unconfined vapor cloud. As the injection height increases, the cloud becomes more uniform; as a result, the temperature and delay time gradients decrease and the spontaneous wave can propagate faster. Furthermore, the possibility of the pulsing behavior of the detonation decreases. On the other hand, as the injection height decreases, the strength of the upper vortex increases and the lower vortex decays faster. Thus, besides shifting, the contour of the detonable range will also rotate and, because of the heating effect of the lower vortex damping, the delay time usually decreases in the regions near the ground. Therefore, there is a trade-off between all effective parameters. With regard to the initial injection conditions used in this work, such as the injection velocity (250 m/s) and the fuel total mass (15 kg), the results show that a height of injection between 0.75 m and 1.5 m is more suitable. As the injection velocity and/or total fuel mass increases, the optimum injection height increases.

The consistency of the numerical results with those of experiment is fairly good. The results of such a study may also be useful for the storage of a fuel, as well as for safety problems.

REFERENCES

1. Bjerketvedt, D., Bakke, J.R. and Wingerden, K.V. "Gas explosion handbook", *J. of Hazardous Materials*, **52**, pp 1-150 (1997).
2. Alekseev, V.I., Dorofeev, S.B., Sidorov, V.P. and Chaivanov, B.B. "Experimental study of large scale unconfined fuel spray detonations", *Prog. Astronaut. Aeronaut.*, **154**, pp 95-104 (1993).
3. Benedick, W.B., Knystautas, R., Lee, J.H.S. and Tieszen, S.R. "Detonation of unconfined large scale fuel spray-air clouds", *Prog. Astronaut. Aeronaut.*, **133**, pp 297-310 (1991).
4. Thomas, G.O. and Jones, A. "Some observations of the jet initiation of detonation", *Combustion and Flame*, **120**, pp 392-398 (2000).
5. Ungut, A. and Shuff, P.J. "Deflagration to detonation transition from a venting pipe", *Combust. Sci. and Tech.*, **63**, pp 75-87 (1989).
6. Lizhong, Y., Weicheng, F., Xiaodong, Z. and Qing'an, W. "Analysis of fire and explosion hazards of some hydrocarbon-air mixtures", *J. of Hazardous Materials*, **A84**, pp 123-131 (2001).
7. Doustdar, M.M., Hosseinalipour, M. and Mazaheri, K. "Numerical study of two-phase unconfined fuel-air cloud characteristics to consider its detonability", *10th Annual Conf. of the CFD Society of Canada*, pp 204-210 (2002).

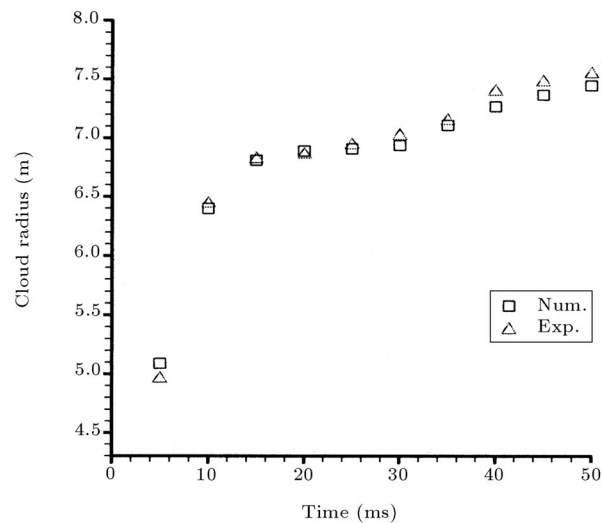


Figure 17. Comparison between the numerical simulation and experiments.

8. Bartenev, A.M. and Gelfand, B.E. "Spontaneous initiation of detonations", *Progress in Energy and Combustion Science*, **26**, pp 29-55 (2000).
9. Khokhlov, A.M., Oran, E.S. and Thomas, G.O. "Numerical simulation of deflagration to detonation transition: The role of shock-flame interactions in turbulent flames", *Combustion and Flame*, **117**, pp 323-339 (1999).
10. Makhviladze, G.M., Roberts, J.P. and Yakush, S.E. "Combustion of two-phase hydrocarbon fuel clouds released into the atmosphere", *Combustion and Flame*, **118**, pp 583-605 (1999).
11. Glass, M.W. "Far-field dispersal modeling for fuel-air explosive devices", *Sandia National Laboratories Report, SAND90-0528* (May 1990).
12. Amsden, A.A., O'Rourke, P.J. and Butler, T.D. "KIVA-II: A computer program for chemically reactive flows with sprays", Los Alamos National Laboratory Report LA-11560-MS (May 1989).
13. Amsden, A.A. "KIVA-3: A KIVA program with block-structured mesh for complex geometries", Los Alamos National Laboratory Report LA-12503-MS (March 1993).
14. Gardner, D.R. "Near-field dispersal modeling for liquid fuel-air explosives", Sandia National Laboratories Report, SAND90-0686 (July 1990).
15. Liu, J.C., Xue, S.S., Zhu, G.S., Zhang, Z.C. and Xie, L.F. "Experimental and numerical study on explosive dispersal and fuel-air cloud", *Proc. of the Colloquium on Gas, Vapor, Hybrid and Fuel-Air Explosions*, Schaumburg, Illinois, pp 341-354 (1998).
16. Kreyszig, E., *Advanced Engineering Mathematics*, 4th Ed., Chap. 20, John Wiley & Sons (1979).
17. Moen, I.O. "Transition to detonation in fuel-air explosive clouds", *J. of Hazardous Materials*, **33**, pp 159-192 (1993).
18. Khokhlov, A.M., Oran, E.S. and Wheeler, J.C. "A theory of deflagration to detonation transition in unconfined flames", *Combustion and Flame*, **108**, pp 503-517 (1997).